

1172

# NATIONAL ADVISORY COMMITTEE FOR AERONAUTICS

APR 30 1947

TECHNICAL NOTE

No. 1113

COLLECTION AND ANALYSIS OF HINGE-MOMENT DATA

ON CONTROL-SURFACE TABS

By Paul E. Purser and Charles B. Cook

Langley Memorial Aeronautical Laboratory  
Langley Field, Va.



Washington

April 1947

NACA LIBRARY  
LANGLEY MEMORIAL AERONAUTICAL  
LABORATORY  
Langley Field, Va.

## NATIONAL ADVISORY COMMITTEE FOR AERONAUTICS

## TECHNICAL NOTE NO. 1113

COLLECTION AND ANALYSIS OF HINGE-MOMENT DATA  
ON CONTROL-SURFACE TABS

By Paul E. Purser and Charles B. Cook

## SUMMARY

Various wind-tunnel data on the hinge-moment characteristics of control-surface tabs have been collected and analyzed. The data, all of which are for plain unbalanced tabs, were obtained from force tests of models in two- and three-dimensional flow and from pressure-distribution measurements on models in two-dimensional flow. Some data that show the effects of Mach number on tab hinge moments for representative conventional and NACA 6-series airfoil sections are presented.

The analysis indicated that present methods of estimating the section values of the slope of the curves of control-surface hinge moment plotted against angle of attack  $ch_{f\alpha}$  and against control-surface deflection  $ch_{f\delta_f}$  over small ranges of angle of attack and deflection could be extended to chord ratios small enough to include the slope of the curve of tab hinge moment plotted against angle of attack  $ch_{t\alpha}$ . Sufficient data were not available to extend the analysis to include the slope of the curve of tab hinge moment against tab deflection  $ch_{t\delta_t}$ , but such an extension should be possible when more tab data are available. The values of the slope of the curve of tab hinge moment plotted against control-surface deflection  $ch_{t\delta_f}$  were found to depend upon the ratio of tab chord to control-surface chord  $c_t/c_f$ , upon the ratio of control-surface chord to airfoil chord  $c_f/c$ , upon the control-surface trailing-edge angle  $\phi$ , and upon the

condition of the gaps at the tab and control-surface hinge lines. An analysis of approximate aspect-ratio corrections (derived from lifting-line theory) for correcting the section values of  $cht_{\delta_f}$  to finite-span values indicated that the correction depended upon  $c_f/c$  and  $c_t/c_f$  as well as upon aspect ratio.

The data available were not sufficient to allow accurate determinations of all the various factors affecting the differences between section and finite-span values of the tab hinge-moment parameters; thus the desirability of obtaining more tab hinge-moment data on finite-span models at larger values of Mach number and of obtaining more complete aspect-ratio corrections to tab hinge-moment characteristics is indicated.

## INTRODUCTION

In an effort to provide satisfactory methods for predicting control-surface characteristics, the NACA has undertaken a program of summarizing, analyzing, and correlating the results of various experimental investigations of airplane control surfaces. This program has provided collections of aileron and tail-surface test data (references 1 and 2), analyses and correlations of the hinge-moment characteristics of control surfaces with internal balances, plain-overhang and Frise balances, beveled trailing edges, shielded and unshielded horn balances and tabs (references 3 to 8), and an analysis of the lift effectiveness of control surfaces (reference 9).

As airplane sizes and speeds increase and as more reliance is placed upon tabs (particularly spring-linked tabs) to provide the final adjustment of control forces, the hinge moment of the tab about its own hinge axis becomes increasingly important. (See references 10 and 11.) The present report therefore presents an analysis and correlation of the available data on tab hinge-moment characteristics.

## COEFFICIENTS AND SYMBOLS

$c_l$	airfoil section lift coefficient ( $l/qc$ )
$\checkmark c_{h_f}$	flap section hinge-moment coefficient ( $h_f/qc_f^2$ )
$\checkmark C_{h_f}$	flap hinge-moment coefficient ( $H_f/qb_f\bar{c}_f^2$ )
$\checkmark c_{h_t}$	tab section hinge-moment coefficient ( $h_t/qc_t^2$ )
$\checkmark C_{h_t}$	tab hinge-moment coefficient ( $H_t/qb_t\bar{c}_t^2$ )

$P_R$  resultant pressure coefficient  $\left(\frac{p_L - p_U}{q}\right)$

where

$l$	airfoil section lift
$h_f$	flap section hinge moment
$H_f$	flap hinge moment
$h_t$	tab section hinge moment
$H_t$	tab hinge moment
$q$	free-stream dynamic pressure
$c$	airfoil section chord
$\checkmark c_f$	flap section chord behind hinge line
$\checkmark \bar{c}_f$	root-mean-square flap chord behind hinge line
$\checkmark c_t$	tab section chord behind hinge line
$\bar{c}_t$	root-mean-square tab chord behind hinge line
$b_f$	flap span
$b_t$	tab span

$p_U$	static pressure on upper surface of airfoil
$p_L$	static pressure on lower surface of airfoil
$\bar{c}_f'$	root-mean-square chord of portion of flap spanned by tab
$\alpha_0$	angle of attack for infinite aspect ratio, degrees
$\alpha$	angle of attack, degrees
$\delta_f$	deflection of flap with respect to airfoil, degrees
$\delta_t$	deflection of tab with respect to flap, degrees
$\angle \phi$	trailing-edge angle, angle included between upper and lower surfaces at airfoil trailing edge, degrees
$\sqrt{A}$	aspect ratio ( $b^2/s$ )
$\sqrt{E}$	Jones' edge-velocity factor (reference 12)
$\lambda$	taper ratio $\left( \frac{\text{Tip chord}}{\text{Root chord}} \right)$
$k$	section tab hinge-moment constant
$K$	finite-span tab hinge-moment constant
$x$	chordwise location of pressure vent measured from airfoil nose
$\tau$	turbulence factor for tunnel
$R$	Reynolds number
$M$	Mach number
$b$	wing span
$y_i$	spanwise location of tab measured from wing root to inboard end of tab
$y_o$	spanwise location of tab measured from wing root to outboard end of tab

## Derivatives:

The subscripts outside of the parentheses denote the factors held constant when the derivative was taken.

$$c_{hf a} = \left( \frac{\partial c_{hf}}{\partial a_o} \right)_{\delta f, \delta t}$$

$$\sqrt{c_{hf a}} = \left( \frac{\partial c_{hf}}{\partial a} \right)_{\delta f, \delta t}$$

$$\sqrt{c_{ht a}} = \left( \frac{\partial c_{ht}}{\partial a_o} \right)_{\delta f, \delta t}$$

$$\sqrt{c_{ht a}} = \left( \frac{\partial c_{ht}}{\partial a} \right)_{\delta f, \delta t}$$

$$c_{hf \delta f} = \left( \frac{\partial c_{hf}}{\partial \delta f} \right)_{a_o, \delta t}$$

$$\sqrt{c_{hf \delta f}} = \left( \frac{\partial c_{hf}}{\partial \delta f} \right)_{a, \delta t}$$

$$c_{ht \delta f} = \left( \frac{\partial c_{ht}}{\partial \delta f} \right)_{a_o, \delta t}$$

$$\sqrt{c_{ht \delta f}} = \left( \frac{\partial c_{ht}}{\partial \delta f} \right)_{a, \delta t}$$

$$\sqrt{c_{ht \delta t}} = \left( \frac{\partial c_{ht}}{\partial \delta t} \right)_{a_o, \delta f}$$

$$C_{ht} \delta_t = \left( \frac{\partial C_{ht}}{\partial \delta_t} \right)_{\alpha, \delta_f}$$

$$P_a = \left( \frac{\partial F_R}{\partial \alpha_0} \right)_{\delta_t, \delta_f}$$

$$P_{\delta f} = \left( \frac{\partial P_R}{\partial \delta f} \right)_{\alpha_0, \delta_t}$$

$$P_{\delta t} = \left( \frac{\partial P_R}{\partial \delta t} \right)_{\alpha_0, \delta_f}$$

$$a_{\delta f} = \left( \frac{\partial a_o}{\partial \delta f} \right)_{c_l, \delta_t}$$

$$\alpha_{\delta t} = \left( \frac{\partial a_0}{\partial \delta t} \right)_{c_l, \delta_f}$$

$$\Delta C_{haLS} \quad \text{lifting-surface theory correction to } C_{ht\alpha} \\ \text{or } C_{hf\alpha}$$

Subscript:

( $\phi = 0$ ) value of the parameter at zero trailing-edge angle

The terms "flap" and "control surface" are used synonymously as a general expression for any movable control surface such as a rudder, elevator, or aileron.

## DATA AND SCOPE

The data upon which the analysis is based were obtained from references 7 and 13 to 23, as well as from

unpublished results of tests made at the Langley and Ames laboratories. The test conditions covered were for models in two- and three-dimensional flow for a range of angles of attack and flap or tab deflection of about  $\pm 4^\circ$  or  $\pm 5^\circ$ . The geometry and other pertinent data for the various models are summarized in tables I, II, and III. The ranges of the various geometric parameters covered by the models are listed in the following table:

Type test	See table	A	$\lambda$	$\phi$ (deg)	$c_f/c$	$c_t/c_f$	Airfoil thickness
Section pressure distribution	I	----	----	9.3 to 30.5	0.10 to 0.50	0.10 to 1.00	0.09c to 0.16c
Section force	II	----	----	7.4 to 25.0	0.18 to 0.40	0.20 to 0.75	0.09c to 0.18c
Finite-span force	III	2.41 to 6.86	1.00 to 0.39	11.5 to 16.7	0.17 to 0.41	0.20 to 0.41	0.08c to 0.18c

## METHODS OF ANALYSIS

### General Approach

Derivation of  $cht_\alpha$  and  $cht_{\delta t}$ .— In order to determine some logical approach to the problem of correlating tab hinge-moment characteristics, a study was made of a previously derived analysis of  $ch_{f\alpha}$  and  $ch_{f\delta f}$  (reference 24). It was found possible to extend the analysis of reference 24 to chord ratios small enough to include tab hinge-moment characteristics ( $cht_\alpha$  and  $cht_{\delta t}$ ).

The results of the analysis of reference 24 (which supersedes that of reference 5) indicated that chord ratio  $c_f/c$  (or  $c_t/c$ ) and trailing-edge angle  $\phi$  were the primary geometric parameters affecting  $ch_{f\alpha}$  (or  $cht_\alpha$ ) and  $ch_{f\delta f}$  (or  $cht_{\delta t}$ ). The results can be expressed by the following formulas:

$$c_{hf_a} = c_{hf_a}(\phi=0) + \frac{dc_{hf_a}}{d\phi} \phi$$

or

$$c_{ht_a} = c_{ht_a}(\phi=0) + \frac{dc_{ht_a}}{d\phi} \phi \quad (1)$$

and

$$c_{hf_{\delta f}} = c_{hf_{\delta f}}(\phi=0) + \frac{dc_{hf_{\delta f}}}{d\phi} \phi$$

or

$$c_{ht_{\delta t}} = c_{ht_{\delta t}}(\phi=0) + \frac{dc_{ht_{\delta t}}}{d\phi} \phi \quad (2)$$

Derivation of  $c_{ht_{\delta f}}$ .— The analysis of  $c_{ht_{\delta f}}$  began with a study of values of  $c_{ht_{\delta f}}$  derived from the experimental data of references 13 to 16 (corrected for tunnel-wall effect) and similar data derived from Glauert's thin airfoil theory (reference 25) as extended by Perring (reference 26). The derivations were made by personnel of the Langley Stability Tunnel Section for use in preparing reference 27. The study indicated that a series of straight lines would result if  $c_{ht_{\delta f}}$  were plotted against  $\frac{c_t}{c_f}$  with  $c_{ht_{\delta f}} = c_{hf_{\delta f}}$  at  $\frac{c_t}{c_f} = 1.0$  as the end point. Such plots permitted derivation of the formula

$$c_{ht_{\delta f}} = c_{hf_{\delta f}} + k \left( 1 - \frac{c_t}{c_f} \right) \quad (3)$$

where  $k$  was a constant for a given value of  $c_f/c$  and was about 10 percent lower for the experimental NACA 0009 airfoil data than for the thin-airfoil-theory data.

## Specific Approach

Pressure-distribution data.— The pressure-distribution data of references 13 to 18 and unpublished data taken at the Langley Laboratory were plotted in terms of the pressure slopes  $P_a$ ,  $P_{\delta f}$ , and  $P_{\delta t}$  against pressure vent locations  $x/c$ . The plots of  $P_a$  were integrated about various chordwise axes to give values of  $ch_{fa}$  (or  $cht_a$ ) and plots of  $P_{\delta}$  were integrated about the flap (or tab) hinge axes to give values of  $ch_{f\delta f}$  (or  $cht_{\delta t}$ ) for various values of  $c_f/c$  (or  $c_t/c$ ). The values of  $ch_{fa}$  (or  $cht_a$ ) and  $ch_{f\delta f}$  (or  $cht_{\delta t}$ ) were then plotted against trailing-edge angle  $\phi$  for the given values of  $c_f/c$  (or  $c_t/c$ ) and the resulting curves extrapolated to  $\phi = 0$  to obtain  $ch_{fa}(\phi=0)$  (or  $cht_a(\phi=0)$ ) and  $ch_{f\delta}(\phi=0)$  (or  $cht_{\delta}(\phi=0)$ ). The slopes of the curves were also measured to obtain  $\frac{dch_{fa}}{d\phi}$  (or  $\frac{dcht_a}{d\phi}$ ) and  $\frac{dch_{f\delta f}}{d\phi}$  (or  $\frac{dcht_{\delta t}}{d\phi}$ ).

Integration of plots of  $P_{\delta f}$  about axes other than the flap hinge axis provided values of  $cht_{\delta f}$  for various values of  $c_t/c_f$  for each value of  $c_f/c$  for which data were available. The resulting values of  $cht_{\delta f}$  were plotted against  $c_t/c_f$  and values of  $k$  were obtained from the slopes of these curves.

Section force-test data.— The values of  $ch_{fa}$ ,  $cht_a$ ,  $ch_{f\delta f}$ ,  $cht_{\delta t}$ , and  $cht_{\delta f}$  obtained from references 19 to 23 and some unpublished data from the Langley Laboratory were used in the same way as the hinge-moment slopes derived from the pressure-distribution data. Individual values of  $k$  derived from the force-test data were more subject to error than those derived from pressure-distribution data because with force-test data there were only two test points through which to draw the line the slope of which defines  $k$ ; whereas with the pressure-distribution data, as many as ten test points were sometimes available.

Finite-span data.— The finite-span data from reference 7 and some unpublished data were used to provide measured values of  $\text{Cht}_\alpha$  and  $\text{Cht}_{\delta t}$  with which to compare calculated values. The calculated values of  $\text{Cht}_\alpha$  and  $\text{Cht}_{\delta t}$  were obtained from the following empirically derived equations:

$$\text{Cht}_\alpha = \frac{A}{AE + 2} \text{cht}_{\alpha(\phi=0)} + \Delta \text{Cht}_{\alpha_{LS}} + \frac{d\text{cht}_\alpha}{d\phi} \frac{A}{A + 2} \phi \quad (4)$$

and

$$\begin{aligned} \text{Cht}_{\delta t} = & \text{cht}_{\delta t(\phi=0)} + a_{\delta t(\phi=0)} \text{cht}_{\alpha(\phi=0)} \left(1 - \frac{A}{AE + 2}\right) \\ & + \frac{d\text{cht}_{\delta t}}{d\phi} \frac{A}{A + 2} \phi \end{aligned} \quad (5)$$

where values of  $\Delta \text{Cht}_{\alpha_{LS}}$  can be obtained from reference 27;  $a_{\delta t(\phi=0)}$  can be obtained from reference 9, and the other factors can be obtained from the present report.

The finite-span data were also used to obtain values of  $\text{Chf}_{\delta f}$  and  $\text{Cht}_{\delta f}$  from which to derive values of  $K$  for use in the formula

$$\text{Cht}_{\delta f} = \text{Chf}_{\delta f} + K \left(1 - \bar{c}_t / \bar{c}_f'\right) \quad (6)$$

It should be noted that models 13, 14, and 16 of table III had balanced flaps. For these models  $\text{Chf}_{\delta f}$  was computed by subtracting from the test data an increment in  $\text{Chf}_{\delta f}$  caused by the balance as computed by use

of reference 4 for models 13 and 14 and from measured balance-chamber pressures for model 16.

So few finite-span data were available that, in an attempt to extend the usefulness of the data, aspect-ratio corrections were derived by means of lifting-line theory to permit conversion of the section  $k$  to finite-span  $K$ . The formula for the conversion was

$$K = k + \frac{\frac{A}{AE + 2}}{1 - \frac{\bar{c}_t}{\bar{c}_f}} \alpha_{\delta f} (cht_{\alpha} - chf_{\alpha}) \quad (7)$$

which indicates that  $K$  varies with aspect ratio and tab chord; whereas  $k$  varied with flap chord and trailing-edge angle. This effect of tab chord means that the curves of  $cht_{\delta f}$  plotted against  $c_t/c_f$  are not straight lines as were the curves of  $cht_{\delta f}$  against  $c_t/c_f$  and that  $K$  rather than being the slope of the curve (as was  $k$ ) is the slope of a straight line drawn from  $chf_{\delta f}$  at  $\frac{c_t}{c_f} = 1.0$  and intersecting the curve at the value of  $c_t/c_f$  under consideration.

## RESULTS AND DISCUSSION

### Correlation of Section Data

Values of  $cht_{\alpha}$  and  $cht_{\delta t}$ .— The results of the correlations of  $cht_{\alpha}$  (or  $chf_{\alpha}$ ) and  $cht_{\delta t}$  (or  $chf_{\delta f}$ ) are presented in figure 1 as plots of  $cht_{\alpha}(\phi=0)$ ,  $dcht_{\alpha}/d\phi$ ,  $cht_{\delta t}(\phi=0)$ , and  $dcht_{\delta t}/d\phi$  against chord ratio  $c_t/c$ .

The data from which figure 1 was derived were obtained under a variety of conditions; but in all cases the tab and flap gaps were sealed and in most cases the combination of Reynolds number, surface condition, and stream turbulence was such that boundary-layer transition was quite probably located at or ahead of  $0.30c$ . The resulting

scatter of data was such that, in reference 24, the mean curves from which figure 1 was derived were within  $\pm 0.001$  of the experimental values of  $ch_{f\alpha}$  and  $ch_{f\delta_f}$  in most cases. Although few data were available for the chord ratios usual for tabs the data in figure 1 should allow similarly accurate estimations of  $cht_{\alpha}$ . For  $cht_{\delta_t}$ , however, sufficient data were not available for such an extension, but it is believed that the method of reference 24 may be used as a guide for additional analysis as more tab data become available.

Values of  $cht_{\delta_f}$ .— Values of  $k$  required in computing  $cht_{\delta_f}$  from equation (3) are presented in figure 2 as plots of  $k$  against  $cf/c$  for various trailing-edge angles and flap and tab-gap conditions. These data show a considerable amount of scatter; consequently, values of  $k$  for given values of  $cf/c$  and conditions of gaps were plotted against trailing-edge angle  $\phi$ . From these cross plots were obtained values of  $dk/d\phi$  of 0.00008 for sealed gaps and 0.00022 for open gaps. These values of  $dk/d\phi$  were used to reduce the  $k$ -values of figure 2 to zero trailing-edge angle and the resulting data are plotted in figure 3. The data indicate that as the gaps at the flap or tab hinges are opened and as the trailing-edge angle is reduced, the values of  $k$  become smaller, which indicates that the values of  $cht_{\delta_f}$  and  $ch_{f\delta_f}$  more nearly approach equality. The same trends are illustrated in figure 4 which presents plots of  $cht_{\delta_f}$  against  $ct/cf$  for sealed tabs on open and sealed plain 0.30c flaps. The plots of figure 4 also indicate that a straight line (constant value of  $k$ ) represents the data fairly well for values of  $ct/cf$  as low as 0.20 with gap sealed even when the flap is equipped with a pronounced bevel. This result is typical of the plots derived from pressure-distribution data.

#### Correlation of Finite-Span Data

Values of  $cht_{\alpha}$  and  $cht_{\delta_t}$ .— The comparisons of measured values of  $cht_{\alpha}$  and  $cht_{\delta_t}$  with values computed from equations (4) and (5) are shown in figure 5. The available data indicate generally satisfactory agreement between measured and computed values of  $cht_{\alpha}$ . For  $cht_{\delta_t}$ ,

however, no lifting-surface theory corrections are available at present and consequently the computed values are considerably more negative than the measured values and also show more scatter than do the values of  $C_{ht\alpha}$ .

Values of  $C_{ht\delta_f}$ . - Values of  $K$  (equation (6)) measured from the finite-span data are plotted against  $\bar{c}_f'/c$  in figure 6. Strictly speaking, the faired line should not appear on figure 6 since all the test points are not for the same aspect-ratio. The line is shown however to indicate more clearly the ranges of  $K$  and  $\bar{c}_f'/c$  for which test data exist. Since values of  $K$  computed from section data by lifting-line theory (equation (7)) show a disagreement with the measured values (fig. 7(a)) there is evidently an additional lifting-surface-theory correction, the value of which is as yet unknown. In the absence of exact values for such corrections the differences between the computed and measured values of  $K$  were plotted against aspect-ratio, and an empirical correction of  $\Delta K = 0.0025 (A - 4.5)$  was derived. This  $\Delta K$  should be added to the value of  $K$  computed by lifting-line theory (equation (7)). The resulting equation is

$$K = k + \frac{\frac{A}{AE + 2}}{\left(1 - \frac{\bar{c}_t}{\bar{c}_f}\right)} \alpha \delta_f (C_{ht\alpha} - C_{hf\alpha}) + 0.0025 (A - 4.5) \quad (8)$$

Values of  $K$  computed from equation (8) are plotted against measured values of  $K$  in figure 7(b). In this case the agreement is improved and it is thus believed that equation (8) presents a correction for  $K$  that is acceptable until more complete lifting-surface-theory computations are made or until more finite-span tab data become available for use in deriving a better empirical correction.

#### Effects of Mach Number

At present very few data are available to show the effects of Mach number and Reynolds number on tab hinge-moment characteristics. Some information, however, has been obtained from pressure-distribution data presented

in reference 17. Increments in  $cht_a$  caused by an increase in Mach number from 0.197 to 0.472 for plain sealed tabs on 0.20c open-gap balanced flaps on NACA 66(215)-216 and NACA 23012 airfoils are shown in figure 8. These data indicate slightly more negative increments in  $cht_a$  as the tab chord is reduced and considerably more negative increments as the trailing-edge angle is reduced for this particular case where there were open gaps through the airfoils some distance ahead of the tab hinge lines.

Values of the tab section hinge-moment constant  $k$  derived from the pressure-distribution data of reference 17 are presented in figure 9. These data indicate a decrease in  $k$  as the Mach number is increased with the greatest decrease in  $k$  occurring for the sealed internal-balance flap on the NACA 66(215)-216 airfoil.

#### CONCLUDING REMARKS

The analysis of available tab hinge-moment data obtained in two- and three-dimensional force tests and in two-dimensional pressure-distribution tests indicated that present methods of estimating the rate of change of flap section hinge-moment coefficient with angle of attack and with flap deflection could be extended, over small ranges of angle of attack and flap deflection, to chord ratios small enough to include the rate of change of tab section hinge-moment coefficient with angle of attack. Indications are that the method can be extended to include the rate of change of tab section hinge-moment coefficient with tab deflection when more tab data are available. The analysis indicated that available lifting-surface theory corrections for the rate of change of tab hinge-moment coefficient with angle of attack will allow reasonable accuracy in converting section data to finite-span data. With regard to the rates of change of tab hinge-moment coefficient with tab deflection and with flap deflection, however, either lifting-surface computations should be made or more data should be obtained in order that corrections (either theoretical or empirical) may be derived for these derivatives. Some data are available and have been presented concerning Mach number effects on tab hinge moments but they are so limited as to be practically useless for design purposes; consequently, it appears quite

desirable to obtain more tab hinge-moment data at large values of Mach number. ✓

Langley Memorial Aeronautical Laboratory  
National Advisory Committee for Aeronautics  
Langley Field, Va.

## REFERENCES

1. Rogallo, F. M.: Collection of Balanced-Aileron Test Data. NACA ACR No. 4A11, 1944.
2. Sears, Richard I.: Wind-Tunnel Data on the Aerodynamic Characteristics of Airplane Control Surfaces. NACA ACR No. 3L08, 1943.
3. Rogallo, F. M., and Lowry, John G.: Résumé of Data for Internally Balanced Ailerons. NACA RB, March 1943.
4. Purser, Paul E., and Toll, Thomas A.: Analysis of Available Data on Control Surfaces Having Plain-Overhang and Frise Balances. NACA ACR No. 14E13, 1944.
5. Purser, Paul E., and Gillis, Clarence L.: Preliminary Correlation of the Effects of Beveled Trailing Edges on the Hinge-Moment Characteristics of Control Surfaces. NACA CB No. 3E14, 1943.
6. Lowry, John G.: Résumé of Hinge-Moment Data for Unshielded Horn-Balanced Control Surfaces. NACA RB No. 3F19, 1943.
7. Lowry, John G., Maloney, James A., and Garner, I. Elizabeth: Wind-Tunnel Investigation of Shielded Horn Balances and Tabs on a 0.7-Scale Model of XF6F Vertical Tail Surface. NACA ACR No. 4C11, 1944.
8. Crandall, Stewart M., and Murray, Harry E.: Analysis of Available Data on the Effects of Tabs on Control-Surface Hinge Moments. NACA TN No. 1049, 1946.
9. Swanson, Robert S., and Crandall, Stewart M.: Analysis of Available Data on the Effectiveness of Ailerons without Exposed Overhang Balance. NACA ACR No. 14E01, 1944.
10. Phillips, William H.: Application of Spring Tabs to Elevator Controls. NACA ARR No. 14H28, 1944.
11. Phillips, William H.: The Use of Geared Spring Tabs for Elevator Control. NACA RB No. 15A13, 1945.

12. Jones, Robert T.: Correction of the Lifting-Line Theory for the Effect of the Chord. NACA TN No. 817, 1941.
13. Street, William G., and Ames, Milton B., Jr.: Pressure-Distribution Investigation of an N.A.C.A. 0009 Airfoil with a 50-Percent-Chord Plain Flap and Three Tabs. NACA TN No. 734, 1939.
14. Ames, Milton B., Jr., and Sears, Richard I.: Pressure-Distribution Investigation of an N.A.C.A. 0009 Airfoil with a 30-Percent-Chord Plain Flap and Three Tabs. NACA TN No. 759, 1940.
15. Ames, Milton B., Jr., and Sears, Richard I.: Pressure-Distribution Investigation of an N.A.C.A. 0009 Airfoil with an 80-Percent-Chord Plain Flap and Three Tabs. NACA TN No. 761, 1940.
16. Ames, Milton B., Jr., and Sears, Richard I.: Determination of Control-Surface Characteristics from NACA Plain-Flap and Tab Data. NACA Rep. No. 721, 1941.
17. Letko, W., and Denaci, H. G.: Wind Tunnel Tests of Ailerons at Various Speeds. V - Pressure Distributions over the NACA 66,2-216 and NACA 23012 Airfoils with Various Balances on 0.20-Chord Ailerons. NACA ACR No. 3K05, 1943.
18. Hoggard, H. Page, Jr., and Bulloch, Majorie E.: Wind-Tunnel Investigation of Control-Surface Characteristics. XVI - Pressure Distribution over an NACA 0009 Airfoil with 0.30-Airfoil-Chord Beveled Trailing-Edge Flaps. NACA ARR No. L4D03, 1944.
19. Holtzclaw, Ralph W., and Crane, Robert M.: Wind-Tunnel Investigation of Ailerons on a Low-Drag Airfoil. III - The Effect of Tabs. NACA ACR No. 4H15, 1944.
20. Sears, Richard I.: Wind-Tunnel Investigation of Control Surface Characteristics. I - Effect of Gap on the Aerodynamic Characteristics of an NACA 0009 Airfoil with a 30-Percent-Chord Plain Flap. NACA ARR, June 1941.

21. Sears, Richard I., and Liddell, Robert B.: Wind-Tunnel Investigation of Control-Surface Characteristics. VI - A 30-Percent-Chord Plain Flap on the NACA 0015 Airfoil. NACA ARR, June 1942.
22. Sears, Richard I., and Purser, Paul E.: Wind-Tunnel Investigation of Control-Surface Characteristics. XIV - NACA 0009 Airfoil with a 20-Percent-Chord Double Plain Flap. NACA ARR No. 3F29, 1943.
23. Gillis, Clarence L., and Lockwood, Vernard E.: Wind-Tunnel Investigation of Control-Surface Characteristics. XIII - Various Flap Overhangs Used with a 30-Percent-Chord Flap on an NACA 65-009 Airfoil. NACA ACR No. 3G20, 1943.
24. Research Department: Summary of Lateral Control Research. Compiled by Thomas A. Toll. NACA TN No. 1245, 1947.
25. Glauert, H.: Theoretical Relationships for an Aerofoil with Hinged Flap. R. & M. No. 1095, British A.R.C., 1927.
26. Perring, W. G. A.: The Theoretical Relationships for an Aerofoil with a Multiply Hinged Flap System. R. & M. No. 1171, British A.R.C., 1928.
27. Swanson, Robert S., and Priddy, E. LaVerne: Lifting-Surface-Theory Values of the Damping in Roll and of the Parameter Used in Estimating Aileron Stick Forces. NACA ARR No. L5F23, 1945.

TABLE I.- INFORMATION REGARDING PRESSURE-DISTRIBUTION-TEST  
MODELS IN TWO-DIMENSIONAL FLOW

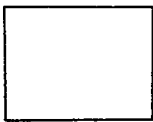
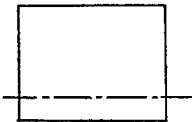
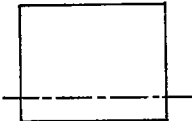
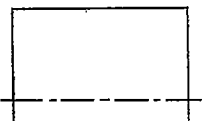
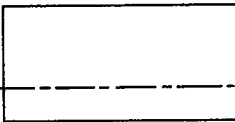

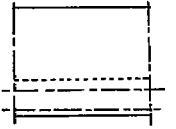


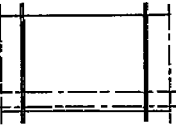


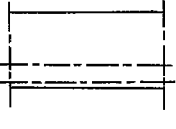

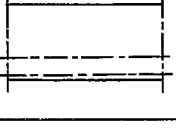

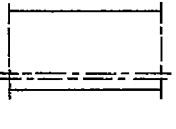

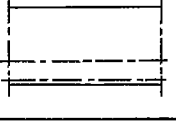


Model	Symbol	Plan form	Airfoil section	$\phi$ (deg)	$c_t/c$	Tab gap	$c_f/c$	Flap gap	Air-flow characteristics	Published reference
1	⊙		NACA 0009	11.6	0 to 0.50	0	0.10 to 0.50	0	$R = 1.77 \times 10^6$ $M = 0.09$ $\tau = 1.93$	13 to 16
2	⊙		NACA 66(215)-216	9.3	0 to 0.20	0	0.20	0 and 0.0055c	$R = 2.8 \times 10^6$ to $6.7 \times 10^6$ $M = 0.20$ to $0.47$ $\tau \rightarrow 1.00$	17
3	⊙		NACA 23012	15.5	0 to 0.20	0	0.20	0.0055c	$R = 2.8 \times 10^6$ to $6.7 \times 10^6$ $M = 0.20$ to $0.47$ $\tau \rightarrow 1.00$	17
4	⊙		NACA 6-series	11.0	0 to 0.225	0	0.225	0.0050c	$R = 6.0 \times 10^6$ $M = 0.14$ $\tau \rightarrow 1.00$	-----
5	△		NACA 0009	25.4 and 30.5	0 to 0.30	0	0.30	0 and 0.0050c	$R = 2.76 \times 10^6$ $M = 0.10$ $\tau = 1.93$	18

TABLE II.-- INFORMATION REGARDING FORCE-TEST MODELS IN  
TWO-DIMENSIONAL FLOW

Model	Symbol	Plan form	Airfoil section	$\theta$ (deg)	$c_t/c_r$	Tab gap	$c_f/c$	Flap gap	$c_{f\delta_f}$	$c_{t\delta_f}$	$c_{t\delta t}$	$c_{t\delta c}$	Air-flow characteristics	Published reference
6			NACA 65,3-018	25.0	0.25	0	0.18	0	-0.0019	0.0020	-0.0022	0.0034	$R = 2.8 \times 10^6$ and $5.1 \times 10^6$ $M = 0.20$ and $M = 0.38$ $T \rightarrow 1.00$	-----
7	 		NACA 66(215)216 $a = 0.6$	9.3 21.7	0.20 .20	0.0008 .0008	0.20 .20	0	-0.0096 -.0050	-0.0044 .0010	-0.0074 -.0059	-0.0026 .0024	$R = 9.0 \times 10^6$ $M = 0.32$ $R = 9.0 \times 10^6$ $M = 0.32$ $T \rightarrow 1.00$	19
8	 		NACA 0009	11.6 11.6	0.20 .20	0.0010 .0010	0.30 .30	0.0010 0	-0.0115 -.0125	-0.0035 -.0035	-0.0061 -.0070	-0.0009 -.0013	$R = 2.76 \times 10^6$ $M = 0.10$ $T = 1.93$	20
9			NACA 0015	19.7	0.20	0	0.30	0	-0.0080	-0.0010	-0.0052	0.0012	$R = 2.76 \times 10^6$ $M = 0.10$ $T = 1.93$	21
10			NACA 0009	11.6	0.75	0	0.20	0	-0.0100	-0.0075	-0.0060	-0.0033	$R = 2.76 \times 10^6$ $M = 0.10$ $T = 1.93$	22
11			NACA 66-009	7.4	0.20	0.0010	0.30	0.0050	-0.0128	-0.0056	-0.0100	-0.0044	$R = 2.76 \times 10^6$ $M = 0.10$ $T = 1.93$	23
12			NACA 0012 (modified)	10.0	0.20	0.0010	0.40	0.0030	-0.0120	-0.0024	-0.0069	-0.0024	$R = 6.0 \times 10^6$ $M = 0.14$ $T = 1.00$	-----

\*Plain flap value estimated from balanced-flap tests.

NATIONAL ADVISORY  
COMMITTEE FOR AERONAUTICS

TABLE III - INFORMATION REGARDING FORCE-TEST MODELS IN  
THREE-DIMENSIONAL FLOW

Model	Symbol	Plan form	Airfoil section		$\bar{p}$ (deg)	A	$\Lambda$	Tab location		$c_{x/cr}$	Tab gap	$c_{r/c}$	Flap gap	$C_{H_{ref}}$	$C_{H_{ref}}$	$C_{H_{ref}}$	$C_{H_{ref}}$	Air-flow characteristics	Published reference
			Root	Tip				$\frac{y_1}{b/2}$	$\frac{y_2}{b/2}$										
13			18-percent thick con- ventional	9-percent thick con- ventional	16.5	6.86	0.625	0.14	0.41	0.375	0	0.167	0.0025c	-0.0060	0.0030	-----	0.0011	$R = 4.0 \times 10^6$ $M = 0.30$ $T \rightarrow 1.00$	-----
14			NACA 0014	NACA 0014	16.0 16.0 16.0 16.0	4.06 4.06 4.06 4.06	1.000 1.000 1.000 1.000	0 0 0 0	0.39 .20 .39 .39	0.408 .395 .395 .406	0 .0062c .0062c .0062c	0.311 .322 .322 .311	0 .0062c .0062c .0062c	-0.0091 -0.0062 -0.0087 -0.0080	-0.0015 -0.0050 -0.0045 -0.0014	-0.0050 -0.0040 -0.0048 -0.0065	-0.0003 -0.0028 -0.0015 -0.0018	$R = 1.67 \times 10^6$ $M = 0.10$ $T = 1.6$	-----
15			Modified NACA 16-series	Modified NACA 16-series	11.5 11.5 11.5 11.5	2.86 2.86 2.86 2.86	0.392 0.392 0.392 0.392	0.34 0.34 0.34 0.34	0.56 0.56 0.56 0.56	0.303 0.305 0.305 0.305	0.0015c 0 0 0	0.320 0.320 0.320 0.320	0 0 0 0	-0.0080 -0.0086 -0.0086 -0.0097	-0.0010 -0.0011 -0.0015 -0.0014	-0.0044 -0.0063 -0.0052 -0.0030	0 0 0 0	$R = 2.30 \times 10^6$ $M = 0.10$ $T = 1.6$	7
16			Modified NACA 651-012	Modified NACA 651-012	16.0 16.0	5.00 5.00	0.500 0.500	0.09 0.09	0.45 0.45	0.200 0.200	0.0010c 0.0010c	0.320 0.320	0 0	-0.0119 -0.0151	-0.0019 -0.0019	-0.0055 -0.0065	0 0.0008	$R = 2.76 \times 10^6$ $M = 0.21$ $T \rightarrow 1.00$ transition free transition fixed at 0.25c	-----
17			NACA 0015	NACA 0009	16.7	4.50	0.500	0.12	0.65	0.200	Open min. gap	0.410	0	-0.0062	-0.0005	-----	0.0005	$R = 4.00 \times 10^6$ $M = 0.05$ $T \rightarrow 1.00$	-----
18			Modified NACA 66-series	Modified NACA 66-series	15.0 15.0	2.41 2.41	0.47 0.47	0.32 0.32	0.58 0.58	0.325 0.325	0.0015c 0	0.325 0.325	0.0035c 0	-0.0045 -0.0045	-0.0010 -0.0014	-0.0060 -----	0.0007 0.0005	$R = 1.51 \times 10^6$ $M = 0.10$ $T = 1.6$	-----

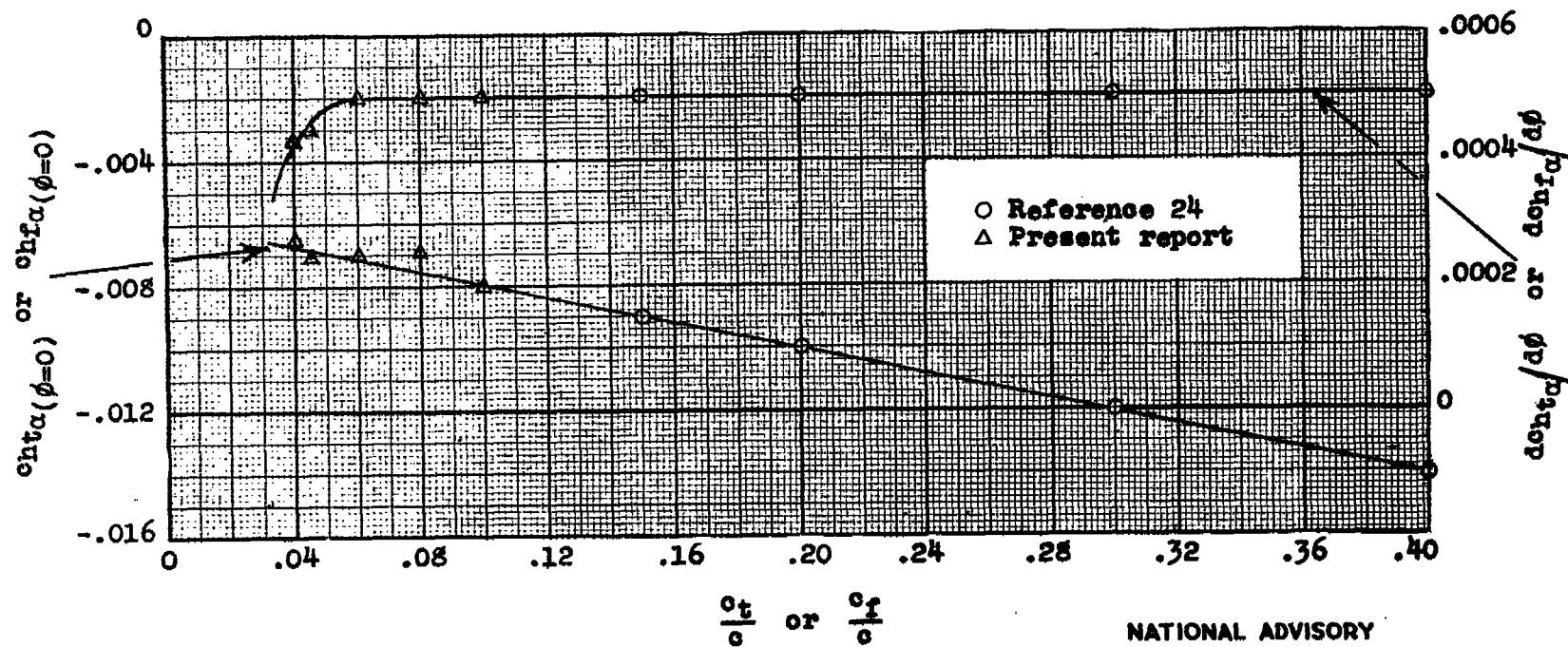
\*Plain-flap value estimated from balanced-flap tests.

$c_{H_{ref}}$ -hinge:



$c_{H_{ref}}$ -hinge:

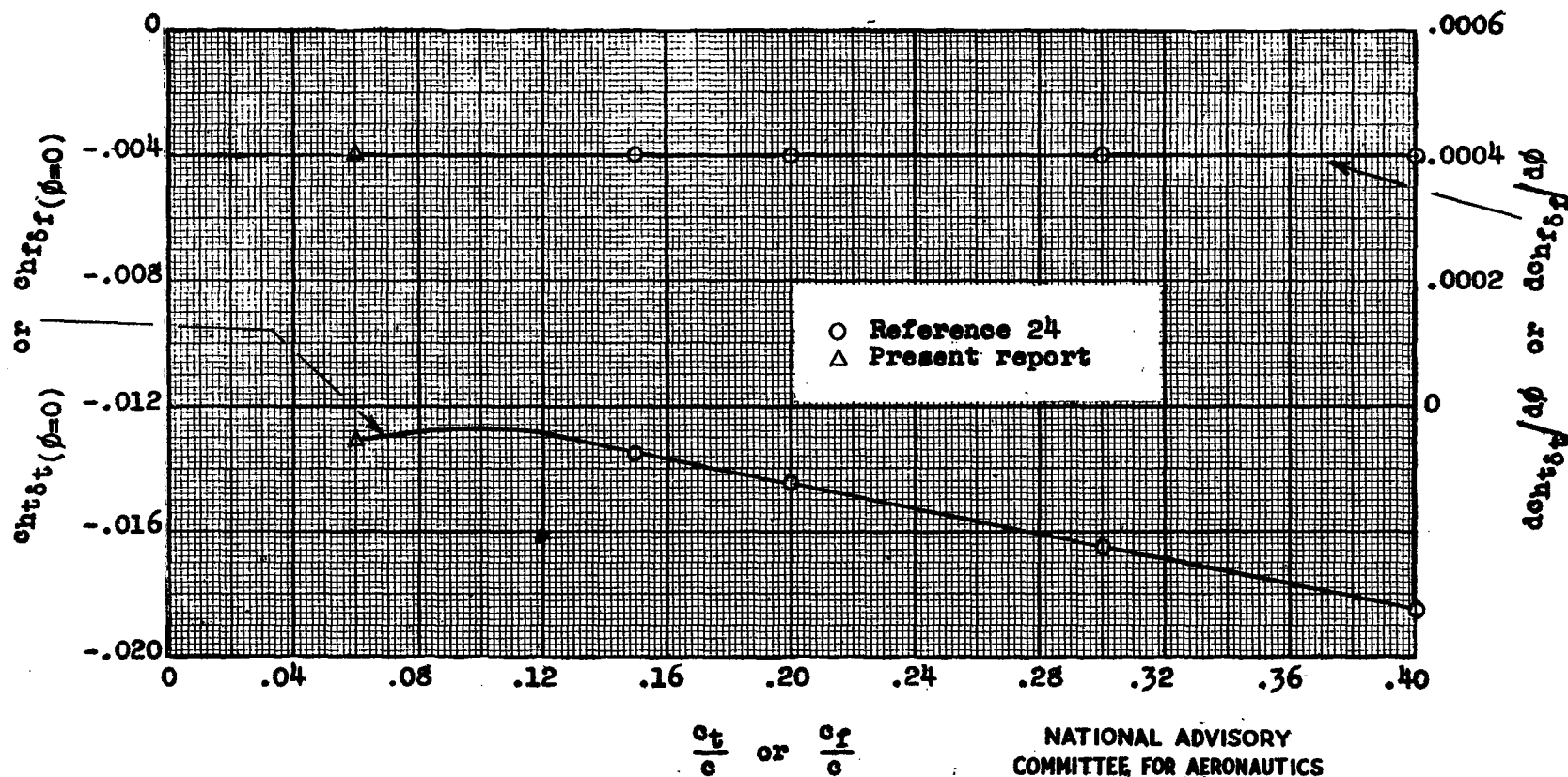




(a) Angle-of-attack slopes.

NATIONAL ADVISORY  
COMMITTEE FOR AERONAUTICS

Figure 1.- Effect of tab or flap chord on the hinge-moment parameters derived from various two-dimensional pressure-distribution and force-test data.



(b) Tab or flap-deflection slopes.

Figure 1.- Concluded.

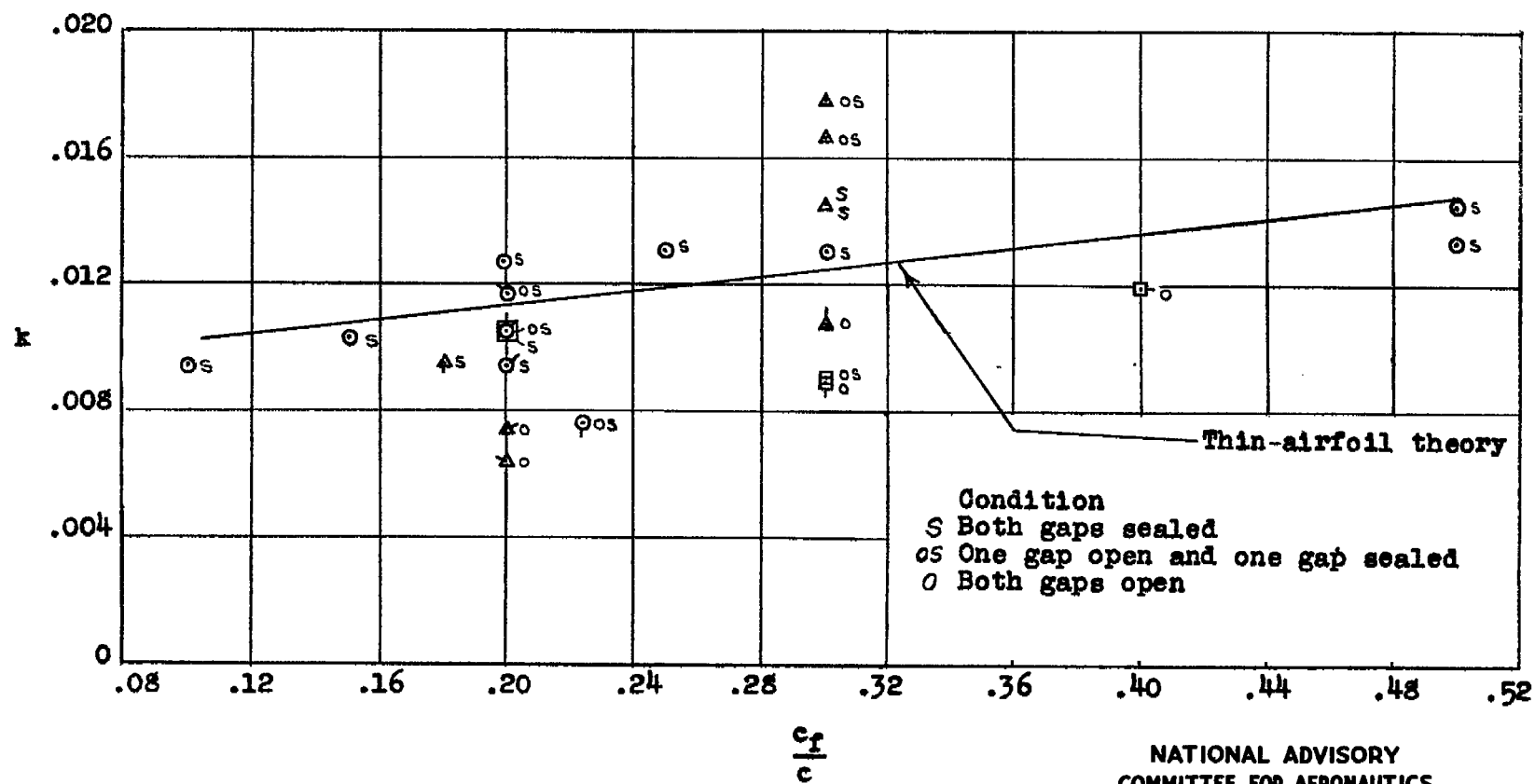


Figure 2.- Variation of tab section hinge-moment constant  $k$  with flap chord ratio  $\frac{c_f}{c}$  for various combinations of flap and tab gap. Symbols refer to models listed in tables I and II.

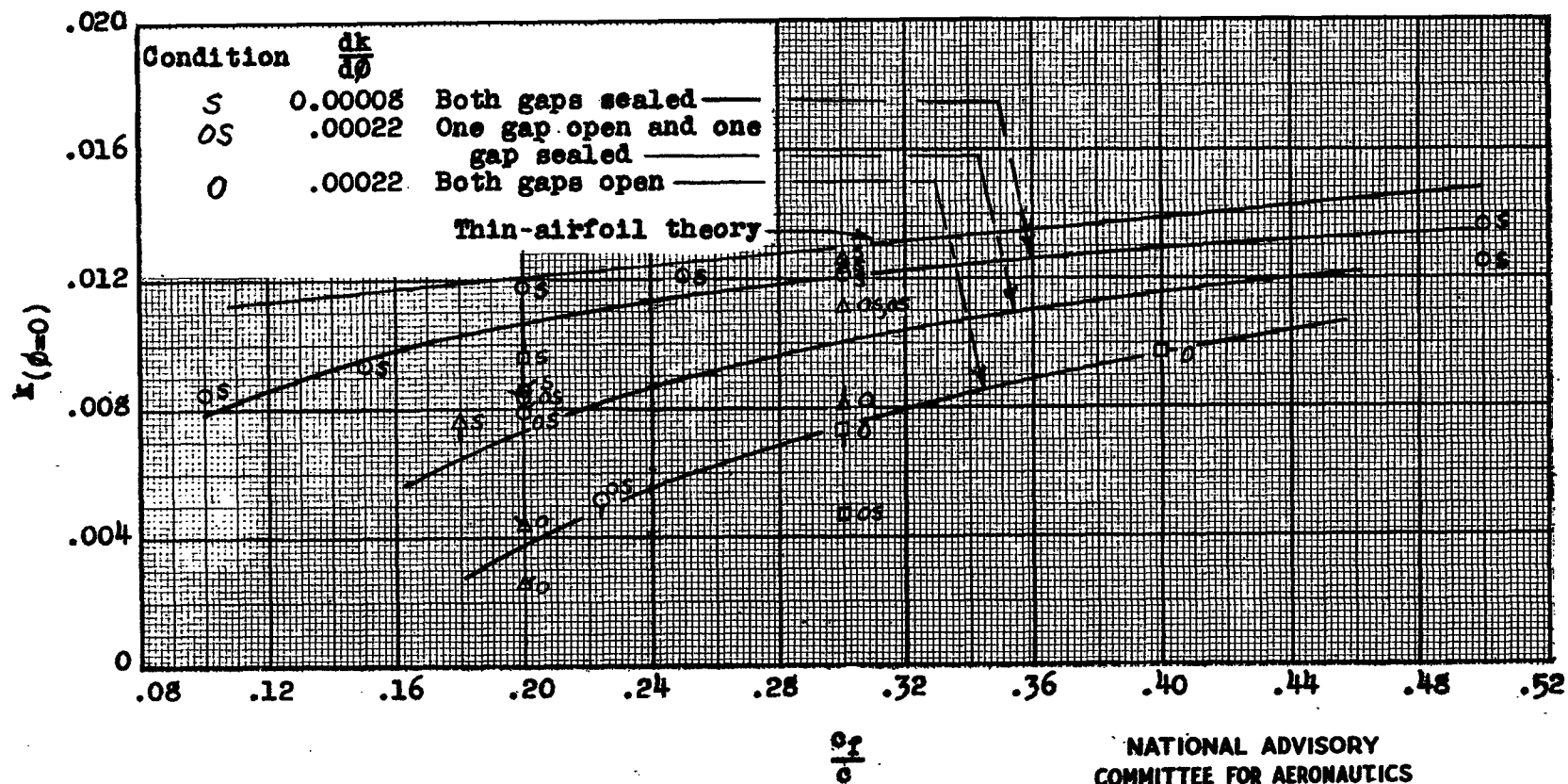


Figure 3.- Variation of tab section hinge-moment constant at  $0^\circ$  trailing-edge angle  $k(\phi=0)$  with flap-chord ratio  $\frac{c_f}{c}$  for various combinations of flap and tab gap. Symbols refer to models listed in tables I and II.

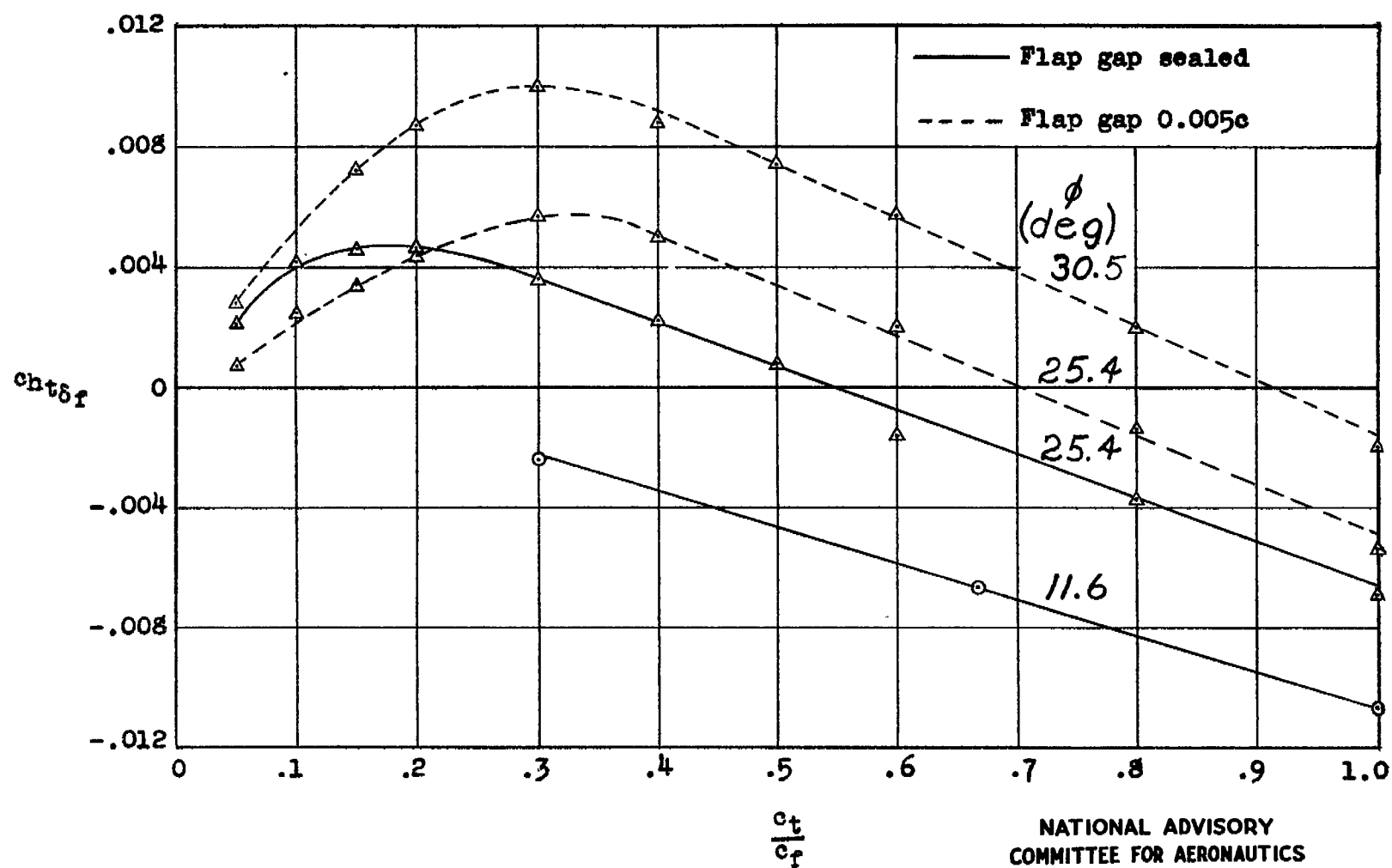


Figure 4.- Effect of trailing-edge angle  $\phi$  on the variation of  $c_{ht\delta f}$  with  $\frac{c_t}{c_f}$  for plain sealed- and open-gap 0.30c flaps on an NACA 0009 airfoil section. Symbols refer to models listed in table I.

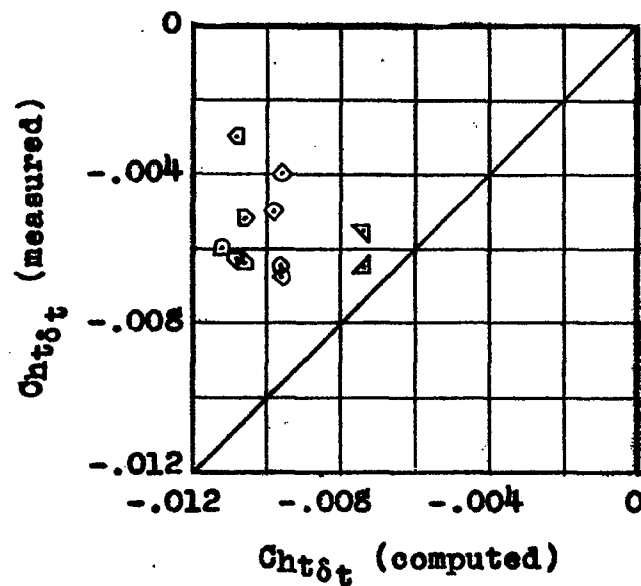
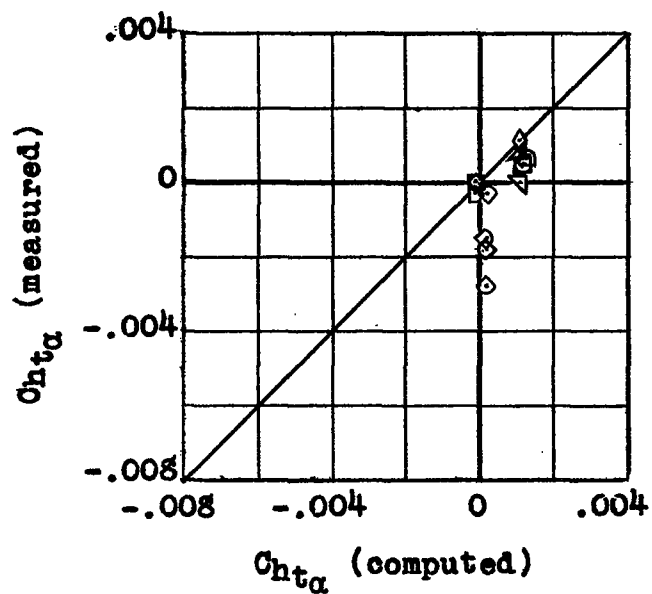


Figure 5.- Comparison of measured and computed values of  $C_{ht\alpha}$  and  $C_{ht\delta_t}$ . Symbols refer to models in table III.

NATIONAL ADVISORY  
COMMITTEE FOR AERONAUTICS

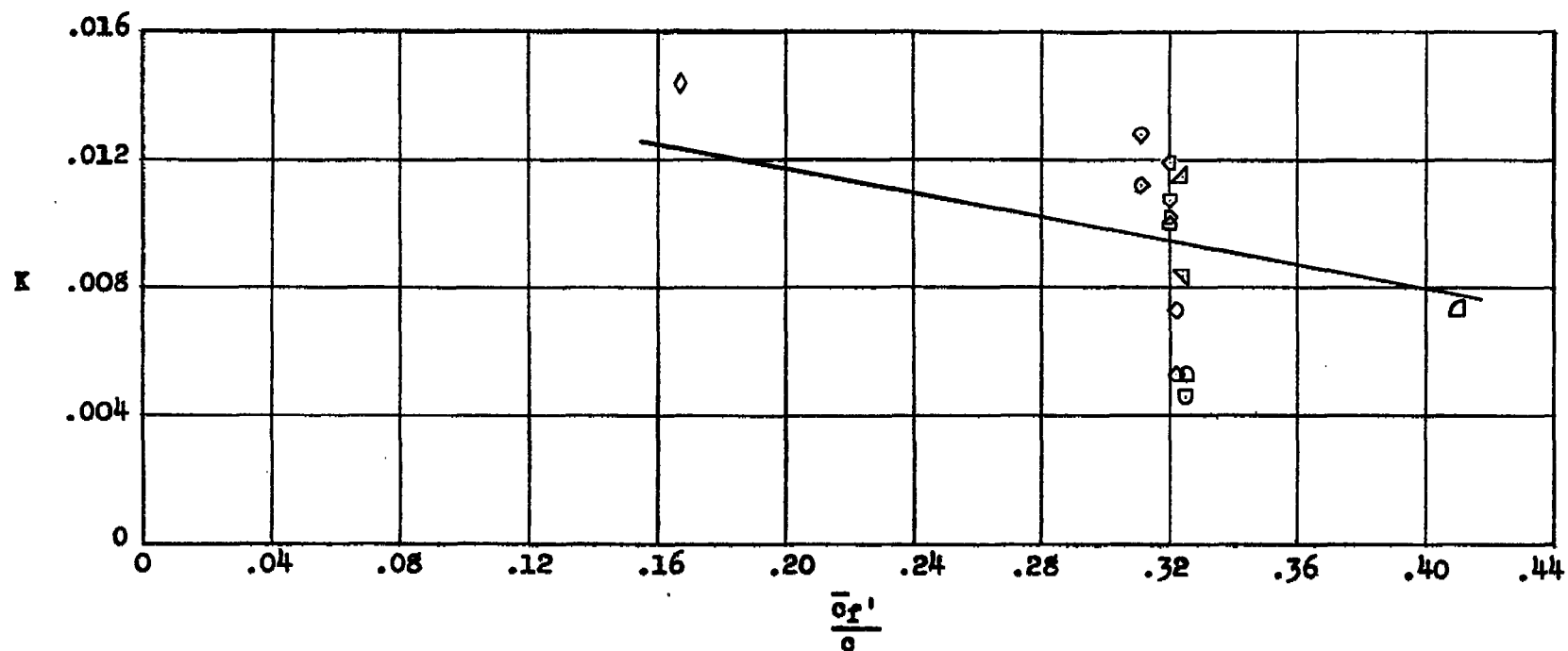
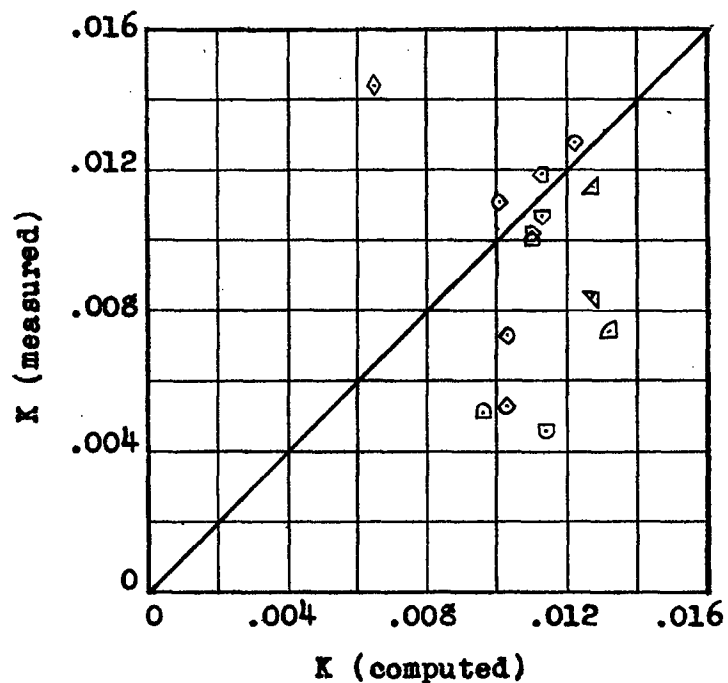
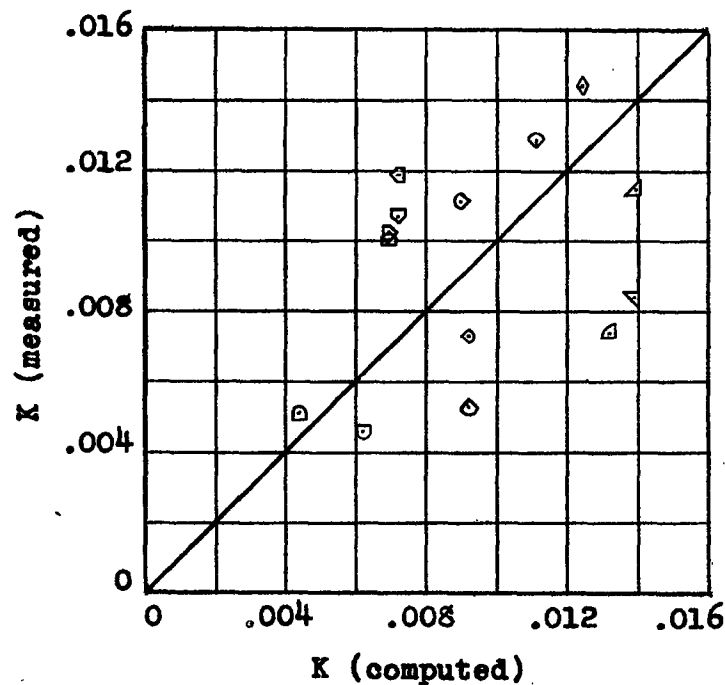


Figure 6.- Measured values of finite-span tab hinge-moment constant  $K$  plotted against flap-chord ratio  $\frac{c_f'}{c}$  for illustrative purposes only. Symbols refer to models in table III.

NATIONAL ADVISORY  
COMMITTEE FOR AERONAUTICS



(a) Lifting-line theory (equation (7)).



(b) Lifting-line theory plus empirical correction (equation (8)).

Figure 7.- Comparison of measured and computed values of the finite-span tab hinge-moment constant  $K$ . Symbols refer to models in table III.

NATIONAL ADVISORY  
COMMITTEE FOR AERONAUTICS

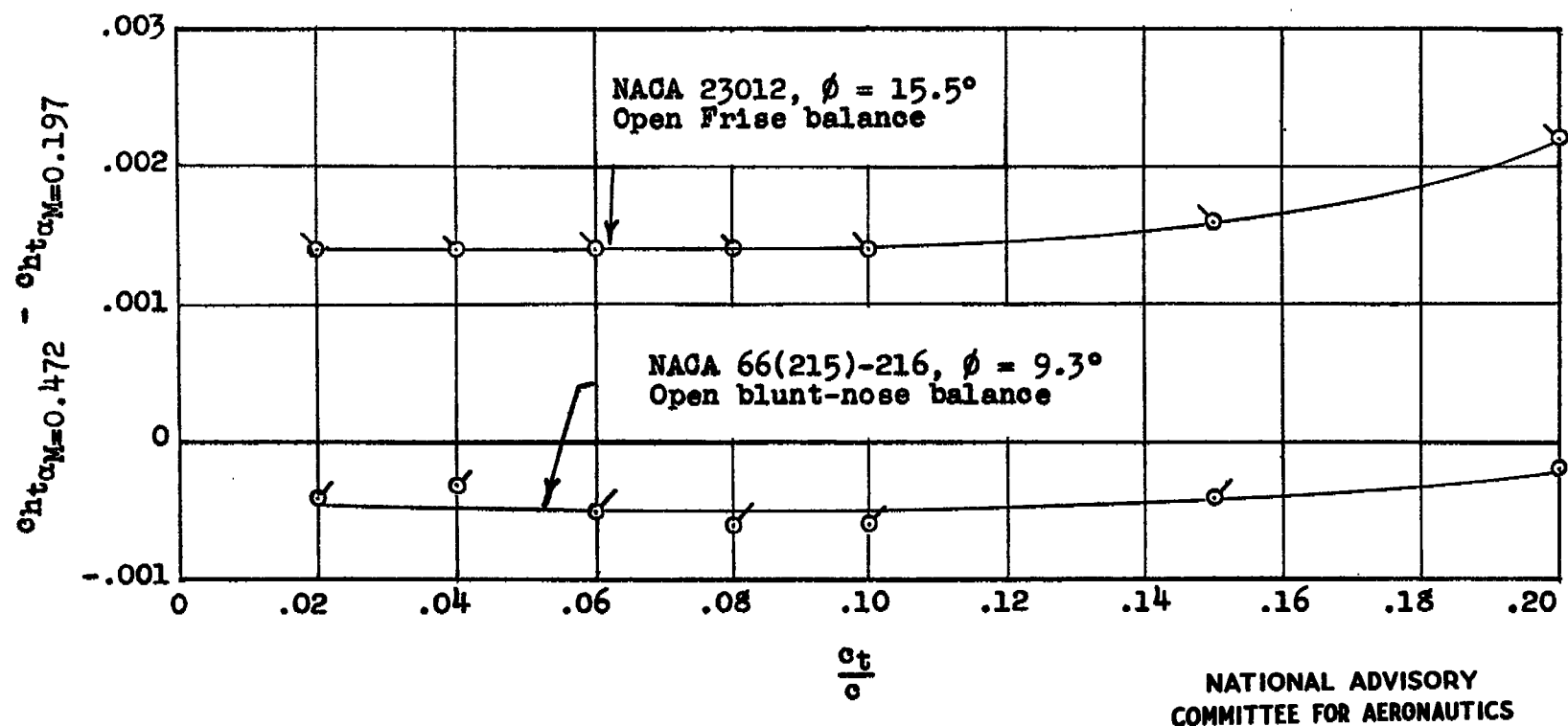


Figure 8.- Effect of tab-chord ratio on the increment in  $C_{ht\alpha}$  resulting from an increase in Mach number for plain sealed tabs on 0.20c open-gap balanced flaps on NACA 23012 and NACA 66(215)-216 airfoils. Derived from pressure-distribution data of reference 17.  $R, 2.8 \times 10^6$  for  $M = 0.197$ ;  $R, 6.7 \times 10^6$  for  $M = 0.472$ .

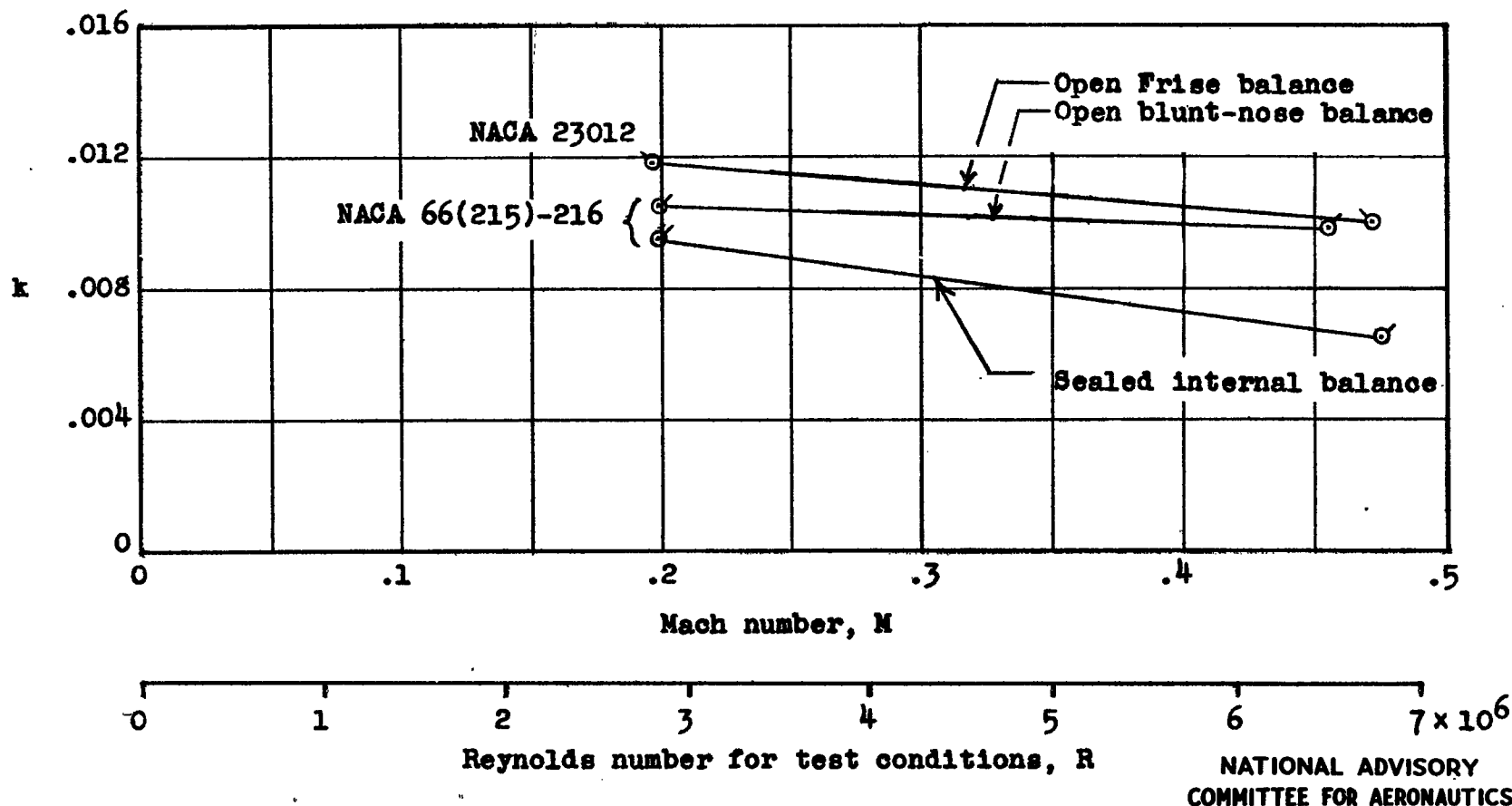


Figure 9.- Variation of section tab hinge-moment constant  $k$  with Mach number and Reynolds number for 0.20c flaps on NACA 66(215)-216 and NACA 23012 airfoil sections. Symbols refer to models listed in table I.